Lu, Xiaohui; Ren, Jianglin; Guo, Lin; Wang, Peifang; Yousefi, Nasser

Article

Improved grass fibrous root algorithm for exergy optimization of a high-temperature PEMFC

Energy Reports

Provided in Cooperation with:
Elsevier

Suggested Citation: Lu, Xiaohui; Ren, Jianglin; Guo, Lin; Wang, Peifang; Yousefi, Nasser (2020) : Improved grass fibrous root algorithm for exergy optimization of a high-temperature PEMFC, Energy Reports, ISSN 2352-4847, Elsevier, Amsterdam, Vol. 6, pp. 1328-1337, https://doi.org/10.1016/j.egyr.2020.05.011

Energy Reports 6 (2020) 1328–1337

Contents lists available at ScienceDirect

Energy Reports

journal homepage: www.elsevier.com/locate/egyr

Research paper

Improved grass fibrous root algorithm for exergy optimization of a high-temperature PEMFC

Xiaohui Lu [a,*], Jianglin Ren [a], Lin Guo [b], Peifang Wang [a], Nasser Yousefi [c]

[a] School of Earth Science and Engineering, Ministry of Education Key Laboratory of Integrated Regulation and Resource Development on Shallow Lakes, Hohai University, Nanjing, 210098, China
[b] Henan Institute of Geological Survey, Zhengzhou, 450001, China
[c] Islamic Azad University, Karaj Branch, Iran

ARTICLE INFO

Article history:
Received 4 April 2020
Received in revised form 10 May 2020
Accepted 14 May 2020
Available online xxxx

Keywords:
Proton exchange membrane fuel cell
Grass fibrous root algorithm
Improved
Exergy analysis
Irreversibility

ABSTRACT

This paper presents an exergy assessment for a proposed power generation system that is used the organic Rankine cycle to recycle the waste heat from a high-temperature proton exchange membrane fuel cell (HT-PEMFC). To do so, mathematical model for the studied PEMFC along with the water management system have been introduced. Parametric analysis has been directed to study the impact of different economic and thermodynamic parameters, like the fuel cell irreversibility, exergy efficiency, and its work. For optimal designing the PEMFC, its parameters have been optimized by considering three objective functions, i.e. irreversibility, exergy efficiency, and its work. The optimization process has been performed based on a new model of fibrous root optimization algorithm improved. Simulation results of the presented algorithm have been compared with empirical results, genetic algorithm, and the basic of fibrous root optimization algorithm. The optimized values of irreversibility, exergy efficiency, work for the proposed algorithm are achieved 0.012, -0.439, and -0.4993, respectively which has the best values compared with the other analyzed algorithms.

1. Introduction

Energy and different ways for access to it, is one of the most important concerns of 21st century. The competition for providing the required energy is not only a concern among the advanced countries, but also it is important for the developing and the third world countries as global communities (Ghadimi, 2012). The rising energy prices of fossil fuels in the last decade, the environmental difficulties and difficulties of using nuclear energy and the limited and non-renewable nature of conventional fuels are some reasons that have expanded research into finding new sources of energy (Fei et al., 2019; Liu et al., 2020; Shamel and Ghadimi, 2016). These resources must have some characteristics, such as easy accessibility, renewability, no environmental pollution, high energy, low cost, easy storage, and economical portability (Eskandari Nasab et al., 2014; Fan et al., 2020). A small group of energy resources currently falls into this category. One of the energies that has been extensively studied for many years is fuel cell energy. A fuel cell is a battery-like device that converts electrochemical energy directly into electricity (Chang et al., 2019; Aghajani and Ghadimi, 2018). The overall structure and the basis of the fuel cell work is consistent with the reactions occurring in a galvanic or voltaic cell, albeit with a slight difference (Fei et al., 2019). The fuel cell simply includes two porous electrodes and a solid or liquid electrolyte that creates these closed orbital components for conducting ions (the same structure of our galvanic cell). But the source of energy in the fuel cell is the hydrogen element. Hydrogen as energy carrier in fuel cell comes from various sources such as petroleum products (about 77%) coal (about 18%), water electrolysis (4%) and (1%) other sources. The major contributors to hydrogen carriers are hydrocarbons that are commonly found in fossil fuels, but the difference in their use in fuel cells is that there are no direct hydrocarbons burning in the machine and electricity generated by hydrogen interactions of Fossil fuel and air oxygen happens without combustion (Cold combustion process). Several kinds of fuel cells have been made that their difference is in their type of electrolyte. In addition, various combinations of fuel and oxidizer as well as anodic and cathode catalysts are also possible. Fuels can be diesel, gasoline, or methanol, and even natural gas and methane. Air, chlorine or dioxide-chlorine can be used as oxidants in the cell.

A popular model of fuel cells is proton-exchange membrane fuel cell (PEMFC). The PEMFC is a good alternative to internal combustion engines in the transmission system. The PEMFC has higher efficiency than the other types of fuel cells with fast

* Corresponding author.
E-mail address: luxiaohui945@163.com (X. Lu).

https://doi.org/10.1016/j.egyr.2020.05.011

Nomenclature

A	Membrane activity
a	ohmic loss
$\dot{E}x$	Exergy ratio (kw)
F	Faradays constant ($Cmol^{-1}$)
h	Enthalpy (J/mol)
I	Irreversibility (kw)
i	Current density (A/cm^2)
i_0	Exchange current density (A/cm^2)
P	Pressure (atm)
$\dot{Q}$	Heat generation
R	Universal gas constant ($1/(\text{mol} \times K^{-1})$)
r_f	Molar flow rate (Kmol/s)
T	Temperature (°C)
$t_{membrane}$	Membrane thickness (cm)
V	Cell potential (v)
V_{rev}	Reversible voltage
V_o	Ohmic voltage
V_a	Activation voltage
V_c	Concentration voltage
W	Power (w)
x	Mole fraction

Greek letters:

α	Transfer coefficients
β	overvoltage constants of the concentration
η	Efficiency
$\lambda_{membrane}$	Membrane water content
μ	Chemical potential (J/mol)
ς	Stoichiometric ratio
$\sigma_{membrane}$	Membrane conductivity ($1/(U^{-1} \times cm^{-1})$)

Subscripts:

A	Anode
Act	Activation
C	Cathode
Ch	chemical
FC	Fuel cell
H_2	Hydrogen
H_2O	Water
in	Inlet
O_2	Oxygen
out	Outlet
ph	Physical
ra	Random value
rev	Reversible
s	Specific entropy, $Jmol^{-1}K^{-1}$

reaction and no contamination. These characteristics make the PEMFC as a popular fuel cell model in different applications. Generally, the mathematical model of the PEMFC is a critical case that should be considered for optimal designing and analysis of the fuel cell (Yu and Ghadimi, 2019; Liu et al., 2017). There are various kinds of works have been done in this category in the literature.

Cao et al. (Gollou and Ghadimi, 2017) introduced an optimal model for the PEMFC stack. The main purpose was to present a developed model of seagull optimization algorithm to achieve the optimal parameters for PEMFC identification. The algorithm developed different mechanisms for increasing the algorithm convergence speed. The results were applied and compared with the empirical data from NedStack PS6 and BCS 500-W. The comparison results indicated that the presented technique gave well results from some other similar algorithms from the literature.

Yu et al. (Aghajani and Ghadimi, 2018) presented a parameter identification for the PEMFC using a developed Elman neural network and a combined version of the World Cup Optimization algorithm and the Fluid Search Optimization algorithm. The method was proposed for modifying the method efficiency for identifying the model parameters. Afterwards, four different operational conditions were adopted for the model analysis. Final results indicated the method excellence toward the others.

Wang et al. (Mirzapour et al., 2019) presented a stacked long–short term memory (S-LSTM) model to fit the PEMFC stack degradation. In addition, the method presents the remaining useful life (RUL) estimation. The hyper parameters of the S-LSTM model were optimized based on a differential evolution algorithm. Simulation results showed that the presented model efficiency in comparison with other compared methods.

Guo et al. (Hosseini Firouz and Ghadimi, 2016) applied energy and exergy analysis for a hybrid HT-PMEFC system along with a two-stage thermoelectric generator (TTEG) by considering the Thomson effect. The paper achieved the relationships between the electric current and the inter-stage temperature of the TTEG and the working current density of HT-PEMFC. Simulation results showed that the proposed HT-PEMFC/TTEG system gives the maximum exergetic efficiency, electric efficiency, and power density compared with the basic HT-PEMFC system.

Nalbant et al. (Hamian et al., 2018) proposed another arrangement for HT-PEMFC to give a satisfying technology for cogeneration usages. The research presented a mathematical model along with energy and exergy analysis based on the principles of electrochemistry and thermodynamics. Finally, some key operating parameters were examined.

When energy has been converted in a PEMFC, a determinative value of heat has been generated. During this process, the most extractable work is called exergy, i.e. exergy determines the reversibility of a process during the enhancing of the entropy. However, exergy does not include system features, it characterizes the system and its environment. The reference state of the system is adopted to measure enthalpy and entropy, and the input energy can be changed by varying different parameters like input mass flow rate, pressure, and temperature. Furthermore, internal energy difference between the inputs and the outputs, and also the mechanical work of the system are the principal cases in exergy calculation (Leng et al., 2018). In other words, exergy is the maximum produced work of a fuel cell (Akbary et al., 2019; Ebrahimian et al., 2018). This research performs an energetic analysis and the effect of its parameters on thermodynamic irreversibility will be implemented (Saeedi et al., 2019; Gao et al., 2019). In this research, a methodology has been introduced an exergy synthesis for optimizing the fuel cell function. A PEMFC unit consists of three distinct parts. Anode (negative electrode), electrolyte and cathode (positive electrode). The way the fuel cell reacts is that the hydrogen (H_2) loses its electron at the anode with the intervention of a catalyst and becomes a proton ion (H^+) and free electron (e^-). The proton moves to the cathode via electrolyte. The electrolyte is a solid or liquid compound designed to allow only the proton (and not the electron) to pass through it. Platinum is usually used as a catalyst in the vicinity of anode or hydrogen ion. The electron is also directed to the cathode through an external circuit (here a wire connected to a light source such as a lamp). The ions and electrons then react with the cathode

to produce oxygen. The movement of electrons over the external circuit generates a current that is usable in electrical devices and the water in the cathode can also be reused. Nickel is usually used as a catalyst at the cathode pole (Kwon et al., 2015). For handling the performance of the fuel cell, diffusion and reaction rates are adopted that must be compatible with together. There are several works that have been introduced about the optimizing the exergy for the fuel cells. These methods are usually categorized into two different classes: empirical-based approaches and mechanistic models (Ehyaei and Rosen, 2019). The optimal identification of the fuel cell parameters are like momentum, heat transfer, mass, and diffusion electrochemical reactions (Haghighi and Sharifhassan, 2016). In addition, analyzing the exergy of the system principally increases the fuel cell efficiency. due to the complexity of these kinds of problems, most of the performed optimization algorithms stuck in the local minimum value that gives a weak or even wrong solution. To resolve this shortcoming, in this paper, a new improved version of Grass Fibrous Root Optimization Algorithm (GRA) has been presented. The objective of this study is to optimize and synthesis of the exergy for a PEMFC based on optimal control of some characteristics of the PEMFC. To do so, the study uses three main objectives in the optimization: the exergy efficiency, the work efficiency, and the thermodynamic irreversibility. The contributions of the paper are summarized below:

- A technique is adopted for Exergy analysis on a PEMFC.
- A modified metaheuristic method is used for the model optimizing.
- The metaheuristic is used for the PEMFC optimal identification.
- The algorithm is validated by metaheuristics.
- The method has compared with three different methods from the literature.

2. System model

For modeling and synthetizing performance of the exergy for the analyzed HT-PEMFC, some considerations have been presented. In the system, the gases are considered ideal and the analyzed fuel cell is considered to be worked under steady-state conditions. Because the value of the produced water is too low, it has been neglected in the evaluations. Here, the kinetic energies and the potential have been neglected. During the exergy calculation, the humidity in the input H_2 and O_2 is ignored. Table 1 indicates the studied PEMFC thermodynamic characteristics (Akkar and Mahdi, 2017).

In the following, by considering the Faraday's constant, we can determine the value of the generated H_2 by electrical current and the value of O_2 generated by the achieved H_2 and humidity quantity. The exergy is a proper economical criterion to analyze the system that depends to the irreversibility, enthalpy, work, and entropy of a system. Here, an optimal designing for exergy based on three functions with some predefined constraints has been introduced. Fig. 1 shows the exergy process in the PEMFC.

As can be seen from Fig. 1, the electrochemical reaction between H_2 and O_2 at the catalyst layer is obtained as follows (Reddy and Jayanti, 2012):

$$H_2 + O \rightarrow H_2O + Heat + Electricity \tag{1}$$

The exergy of the fuel cell during the operation, mass, and heat is as follows:

$$\sum \dot{E}x_{in} = \sum \dot{E}x_{out} + \dot{I} \tag{2}$$

Table 1
Thermodynamic characteristics of the considered HT-PEMFC (Akkar and Mahdi, 2017).

Parameter	Value	Unit
The temperature for humidification of the feed gases	28	°C
O_2 utilization ratios	50	%
H_2 utilization ratios	80	%
The thickness for the membrane	0.018 and 0.022	cm
The current density range	[0.02, 1.2]	A × cm^2
The temperature of the dead state	25	°C
Dead state pressure	1	atm
Heat loss ratio (rHL)	20	%
The pressure of the Exergy for the analysis	1, 2 and 3	atm
Operating temperatures of the cells	119.85, 139.85, 159.85 and 179.85	°C

$$\sum \dot{E}x^{in}_{mass} = \sum \dot{E}x_{work} + \sum \dot{E}x^{out}_{mass} - \sum \dot{E}x_{Heat} + \dot{I}_{FC} \tag{3}$$

And the exergy value for the input and the output of the system are:

$$\sum \dot{E}x^{in}_{mass} = \dot{E}x^{in}_{O_2} + \dot{E}x^{in}_{H_2} = \left(\dot{r}_f \times ex\right)^{in}_{H_2} + \left(\dot{r}_f \times ex\right)^{in}_{O_2} \tag{4}$$

$$\sum \dot{E}x_{mass,out} = \dot{E}x^{out}_{O_2} + \dot{E}x^{out}_{H_2} + \dot{E}x^{out}_{H_2O} = \left(\dot{r}_f \times ex\right)^{in}_{H_2} + \left(\dot{r}_f \times ex\right)^{in}_{O_2} + \left(\dot{r}_f \times ex\right)^{in}_{H_2O} \tag{5}$$

There are several parameters that are adopted for determining the exergy. For instance, potential exergy, kinetic exergy, physical exergy, and chemical exergy. The physical and chemical exergies can be considered by the following (Ishihara et al., 2004):

$$Ex = \underbrace{\sum_j x_j E^{CH}_j + RT_0 \sum_j x_j \ln x_j}_{Ex^{CH}} + \underbrace{(h - h_0) - T_0(s - s_0)}_{Ex^{PH}} \tag{6}$$

The rate of molar flow for O_2, H_2, and the produced water are achieved as follows (Reddy and Jayanti, 2012):

$$\dot{n}^{out}_{H_2O} = \frac{1}{2} \times i \times F^{-1} = \dot{n}^{reacted}_{O_2} = 2\dot{n}^{reacted}_{O_2} \tag{7}$$

$$\dot{n}^{in}_{H_2} = \dot{n}^{reacted}_{H_2} + \dot{n}^{out}_{H_2} \tag{8}$$

$$\dot{n}^{in}_{O_2} = \dot{n}^{reacted}_{O_2} + \dot{n}^{out}_{O_2} \tag{9}$$

The following equation describes the wasted exergy over the work (Reddy and Jayanti, 2012):

$$\dot{W}_{FC} = \sum \dot{E}x_{work} \tag{10}$$

And the Nernst equation adopted for obtaining the reversible cell voltage is as follows (Lee et al., 2004):

$$V_r = 1.2 + 43.1 \times 10^{-5} \times T_{FC} \times \left[\ln\left(P_{H_2}\right) + \ln P_O\right] - 85 \times 10^{-5}\left(T_{FC} - 298.15\right) \tag{11}$$

Furthermore, the partial pressure of the H_2 and the O_2 are obtained as follows (Amphlett et al., 1995):

$$P_{H_2} = \frac{1 - \frac{P_{sat}}{P_A}}{1 + \left(\frac{x_A}{2}\right) \times \left(1 + \frac{\varsigma_A}{(\varsigma_A - 1)}\right)} \times P_A \tag{12}$$

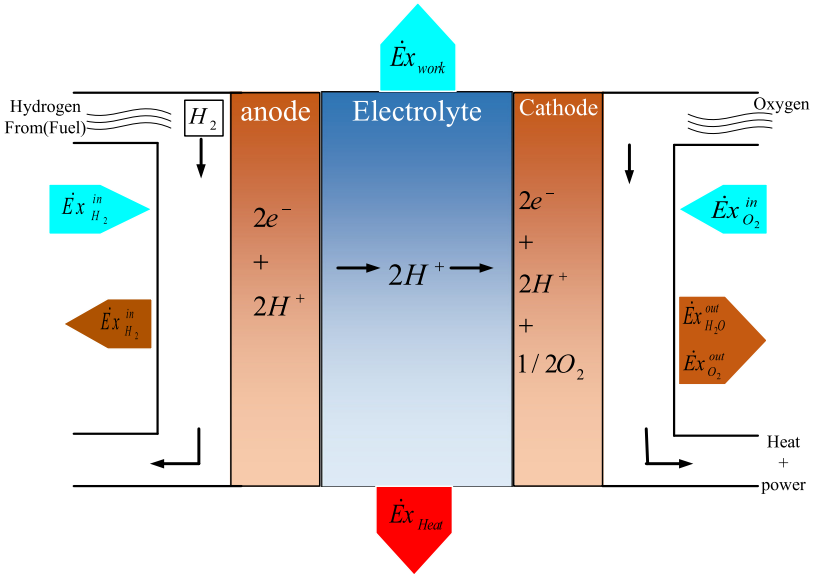

Fig. 1. The PEMFC exergy balancing.

$$P_{O_2} = \frac{1 - \frac{P_{sat}}{P_C}}{1 + \left(\frac{x_C}{2}\right) \times \left(1 + \frac{\varsigma_C}{(\varsigma_C - 1)}\right)} \times P_C \tag{13}$$

The irreversibility reduces the voltage value of the real cell voltage than the equilibrium state. in this study, ohmic loss, activation loss, and concentration loss are considered and modeled that are consequently given below (Rowe and Li, 2001):

$$V_O = t_{membrane} \times i \times \left[(0.005 \times \lambda_{membrane} - 0.003)\, exp\left(4.2 - T_{FC}^{-1}\right)\right]^{-1} \tag{14}$$

$$V_a = \left(\frac{\alpha_A + \alpha_C}{\alpha_A \times \alpha_C}\right) \times \frac{RT_{FC}}{F \times r_f} \times \ln\left(\frac{i}{i_0}\right) \tag{15}$$

$$V_C = i \times \left(\beta_1 \times \frac{i}{i_{max}}\right)^{\beta_2} \tag{16}$$

where,

$$\lambda_{membrane} = \begin{cases} 0.043 + 17.81 \times a - 39.85 \times a^2 - 39.85 \times a^3 & 0 < a \le 1 \\ 14 + 1.4 \times (a - 1) & 1 < a \le 3 \end{cases} \tag{17}$$

and i_0 stands for the exchange current density as follows (Alberro et al., 2015):

$$i_0\,(T) = 10.8 \times 10^{-22} \times exp\,(0.086 \times T_{FC}) \tag{18}$$

The ohmic loss model is as follows (Berning et al., 2002):

$$a = \frac{x_{H_2O} \times P}{P_{sat}} \tag{19}$$

The constants for the overvoltage concentration (β_1 and β_2) are obtained as follows (Haghighi and Sharifhassan, 2016):

$$\beta_1 = \begin{cases} if\ \frac{P_{O_2}}{0.12} + P_{sat} < 2atm \\ (71.6 \times 10^{-5} \times T_{FC} - 0.62)\left(\frac{P_{O_2}}{0.12} + P_{sat}\right) + (1.68 - 14.5 \times 10^{-4} \times T_{FC}) \\ else \\ (86.6 \times 10^{-6} \times T_{FC} - 0.07)\left(\frac{P_{O_2}}{0.12} + P_{sat}\right) + (0.54 - 16 \times 10^{-5} \times T_{FC}) \end{cases} \tag{20}$$

In addition, the fuel cell consuming work, i.e. $\dot{W}_{FC}$ based on Akkar and Mahdi (2017) is considered by the following:

$$\dot{W}_{FC} = V\,(i) \times i = i \times [V_{rev} - V_O - V_a - V_C] \tag{21}$$

Therefore, the exergy for the heat loss is obtained by the following (Alberro et al., 2015):

$$\sum \dot{E}x_{Heat} = r_{HL} \times \dot{Q}_{FC} \tag{22}$$

where, $\dot{Q}_{FC}$ stands for the heat generation in the fuel cell and is obtained by the following:

$$\dot{Q}_{FC} = \dot{Q}_{irrev} + \dot{Q}_{rev} \tag{23}$$

where (Alberro et al., 2015):

$$\dot{Q}_{irrev} = \left(-V_{Cell} - \frac{\Delta G_T}{F \times r_f}\right) \times i \tag{24}$$

$$\dot{Q}_{rev} = -\frac{i \times T_{FC} \times \Delta S_T}{F \times r_f} \tag{25}$$

where, ΔG_T represents the difference of the Gibbs free energy and ΔS_T stands for the entropy change and is obtained as follows (Tian et al., 2020):

$$\Delta S_T = 12414.8 - 9967.35 \times \ln T_{FC} \tag{26}$$

With regardless of the amount of the generated water by the electrolyte, the enthalpy of water generation can be achieved as follow (Akkar and Mahdi, 2017):

$$\Delta H_{g,T} = \Delta H_i^f - \Delta H_T^{vap} \tag{27}$$

where,

$$\Delta H_T^{vap} = 68260.58 + 3.70 \times 10^{-4} \times T_{FC}^3 - 0.48 \times T_{FC}^2 - 152.43 \times T_{FC} \quad (28)$$

And the overall produced heat by a PEMFC is as follows (Akkar and Mahdi, 2017).

$$\dot{Q}_{FC} = -V_{Cell} \times i - \frac{\Delta H_{g,T} \times i}{F \times r_f} \quad (29)$$

Therefore, the thermodynamic irreversibility of the system will be as follows (Akkar and Mahdi, 2017):

$$\dot{I}_{FC} = \left(\sum \dot{E}x_{mass,in} + \sum \dot{E}x_{Heat}\right) - \left(\sum \dot{E}x_{mass,out} + \sum \dot{E}x_{work}\right) \quad (30)$$

And the exergy performance of the fuel is formulated as follows (Akkar and Mahdi, 2017):

$$\eta_{exergy} = \frac{\dot{W}_{FC}}{\dot{E}x_{mass,in}} \quad (31)$$

3. Improved Grass Fibrous Root Optimization Algorithm

Generally speaking, in solving optimization problems, the problem we face has infinite solutions which make us to find the best solution among them. Indeed, different search mechanisms have been performed to these problems and are of the same kind and as such, the algorithms are so useful that explore a large part of the answers to achieve the final solution. The best and most efficient algorithms must have a number of features. For example, high exploration and exploitation that classical optimization algorithms often lack these capabilities in a balanced way. For instance, they do not have the capability of Global search to extract. The mechanism of such algorithms is Local search. Random search algorithms also have a good global search but ultimately cannot achieve the required convergence. In fact, the way in which these algorithms operate intelligently and ultimately converge is the same as meta-evolutionary and evolutionary algorithms. There are different types of metaheuristics which have been proposed in the field of optimization, such as: pigeon-inspired optimization algorithm (Springer et al., 1991), quantum invasive weed optimization (QIWO) (Cui et al., 2019), Emperor Penguin Optimizer (EPO) (Razmjooy and Ramezani, 2014), world cup optimization (WCO) (Dhiman and Kumar, 2018; Bandaghiri et al., 2016; Razmjooy et al., 2017; Shahrezaee, 2017), Collective Animal Behavior (CAB) (Tian et al., 2020), states of matter search (SMS) (Cuevas et al., 2020), and Grass Fibrous Root Optimization Algorithm (GRA) (Cuevas et al., 2018). The common point of these algorithms is to refer to a natural and real phenomenon or social reactions. For example, the QIWO algorithm is derived from invasive growth of the weeds, and the WCO is inspired by the social and humankind challenges to achieve the champion cup, which makes these phenomena a mathematical model and a problem-solving method. In 2017, Akkar and Mahdi (Cuevas et al., 2018) introduced a new metaheuristic algorithm based on the fibrous root system of the grass. The GRA is significantly inspired by the grass plants regeneration, progress, and their fibrous root system. The grass plants are basically replicated based on two procedures. The first one is based on the subterranean stems that is often performed underground by sending out roots and shooting the nodes that is called rhizomes. The second procedure is based on the stems which grow below the surface. The mentioned procedures are continuously developing the secondary roots to replace the vanished primary roots. The hair roots have been produced by the secondary roots. The explained roots are often adopted for local and global searching of the mineral and the water resources. These mechanisms are utilized to model the optimal searching of the GRA. This algorithm gives two different procedures for global search based on the survived grasses and the best achieved grass developed and reproduced. Besides, the local has also two different searching methods including secondary hair roots and regenerated secondary roots. The following subsection, explains briefly about the basic and the improved model of GRA.

3.1. Mathematical model of GRA

The GRA algorithm, just like other metaheuristics, starts by an initial population swarm (grass swarm) that is generated randomly and uniformly in the solution space that is initiated by seeding process (pop). After starting the optimization process, a new population (Pop_{New}) has been generated that is limited in the range $Pop^L_{New} \leq Pop_{New} \leq Pop^H_{New}$, where Pop^L_{New} and Pop^H_{New} represent the lower and the upper ranges of the population variables. The new swarm contains some parameters, such as the best value (G_{best}):

$$G_{best} = \min\left(f\left(swarm\right)\right) \in R^d \quad (32)$$

where, d describes the problem dimension, and f stands for the mean square error (MSE) function.

Another element for the Pop_{New} is the number of grasses (Gr) that is obtained by the G_{best} by *stolons* that are often deviated by the basic grass (Gr_N) including a step size less than Pop^H_{New} as follows:

$$Gr = \left\| (0.5 \times pop) \times \left(\frac{Avg\ (MSE)}{Avg\ (MSE) + min\ (MSE)}\right)\right\| \quad (33)$$

where, Avg and the mindescribe the average value and the minimum value, respectively.

It can be observed that the maximum generated new grass branches are equal to $(0.5 \times pop)$ and obtained when the minimum of MSE is too small. The final mechanism of the Pop^H_{New} is the new grass equal to $(pop–Gr-1)$ that is deviated randomly by the survived best initial grasses (S_{de}). All the new branch grasses deviated by the G_{best} are considered as follows:

$$Gr_N = ones\left(Gr, 1\right) \times G_{best} + 2 \times \max\left(Pop^H_{New}\right) \times \left(\sigma\ \left(Gr, 1\right) - 0.5\right) \times G_{best} \quad (34)$$

And the survived best initial grasses are formulated as follows:

$$S_{de} = Gr_N + 2 \times \max\left(Pop^H_{New}\right) \times \left(\sigma\ \left(pop–Gr-1, 1\right) - 0.5\right) \times Pop^H_{New} \quad (35)$$

where, σ stands for a random value between 0 and 1, $ones\ (.)$ determines the one's column vector, and Gr_N describes the $(pop–Gr-1)$ highest MSE initial population. The new population (Pop_{New}) can be also modeled as follows:

$$Pop_{New} = [G_{best}; Gr_N; S_{de}] \quad (36)$$

The new regenerated population (Pop_{New}) have been evaluated to obtain the minimum valued MSE grass and limited it in the range Pop^L_{New} and Pop^H_{New}. Here, if new G_{best} gives better value than the previous one, it will be substituted by the best new grass (solution), else, the absolute rate of decrease in MSE has been evaluated. If the rate gives less value than or equal to a predefined tolerance value (ε), a global stack ($stack_g$) has been increased and after the $stack_g$reached to its maximum predefined value, then the next local search starts as follows:

$$M = \min_{i=1,\ldots,pop}\left(MSE\right) \quad (37)$$

$$best_{min} = \min_{j=1,\ldots,iter}(M) \tag{38}$$

$$\left|\frac{\min_{i=1,\ldots,pop}(MSE) - G_{best}}{\min_{i=1,\ldots,pop}(MSE)}\right| \leq \varepsilon \tag{39}$$

As before mentioned, there is also local search mechanism in the optimization that contains two parts, hair roots loop and secondary roots loop. The secondary roots are defined by random numbers which will have a number of hair roots equal to d. The updating model of hair root location equal to the secondary roots number (S) is given below.

$$m_{G_{best}}(1,i) = Avg(G_{best}) + G_{best}(1,i) + C_2 \times (\sigma - 0.5) \tag{40}$$

$$C = [C_1, C_2, \ldots, C_{10}] \tag{41}$$

$$C_2 = C \times (1 + (\|\sigma \times 10\|)) \tag{42}$$

$$i = 1, 2, \ldots, d, k = 1, 2, \ldots, S \tag{43}$$

where, $m_{G_{best}}$ describes the locally modified G_{best}, $S \in [0, d]$ stands for the number of secondary generated roots, C describes the analyzed step size vector equation, and C_2 will be a random element of C. If the calculated $m_{G_{best}}$ gives a value less than the G_{best} value, it will be replaced by it, otherwise, MSE absolute rate of decreasing has been evaluated. if the rate is less than ε, then the local stack counter ($stack_l$) will be increased by one, if $stack_l$ gives the maximum predefined value, the hair root loop will be stopped and a new secondary root loop has been started. At the final of each iteration, the stopping criteria (ε_{SC}) will be checked.

3.2. Improved Grass Fibrous Root Optimization Algorithm (IGRA)

However, GRA gives good results in optimization, it has a big drawback in providing a proper convergence, i.e. it has premature convergence for some problems. To resolve this problem, two mechanism have been adopted that are explained in the following:

The first mechanism is Opposition-Based Learning (OBL). The OBL is a technique based on the oriental philosophy conception (Tizhoosh, 2005). By considering the OBL mechanism, opposite positions are obtained based on candidate solutions that helps to enhance the exploration in the algorithm to escape from the local optima for selecting the best solution for the next-generation candidate. Let us consider an integer, x in the range $x\epsilon[x_l, x_u]$. $\bar{x}$ is the opposite value of the integer x and can be formulated as follows:

$$\bar{x} = x_l + x_u - x \tag{44}$$

With extending the above equation into n dimensions,

$$\bar{x}^i = x_l^i + x_u^i - x^i \tag{45}$$

where, $x, \bar{x} \in \mathbb{R}^n$.

After optimization, the best grass in the range x and $\bar{x}$ obtained from the objective function has been extracted and saved as the main solution candidate and the other has been removed, i.e. if $f(x) > f(\bar{x})$, $\bar{x}$ will be stored and x will be removed and if $(x) < f(\bar{x})$, x will be stored and $\bar{x}$ will be removed. Here, 60% of the population has been generated by the OBL mechanism. There is also a filtering for removing

In this step, the out-of-range solutions to obtain the optimal values.

The second mechanism is Lévy flight (LF) that is regularly adopted for developing metaheuristics (Choi and Lee, 1998). Random walk technique is the heart of the LF mechanism which is used for modifying the search capability. The mathematical model of LF mechanism is given below:

$$LF(w) \approx w^{-(\tau+1)} \tag{46}$$

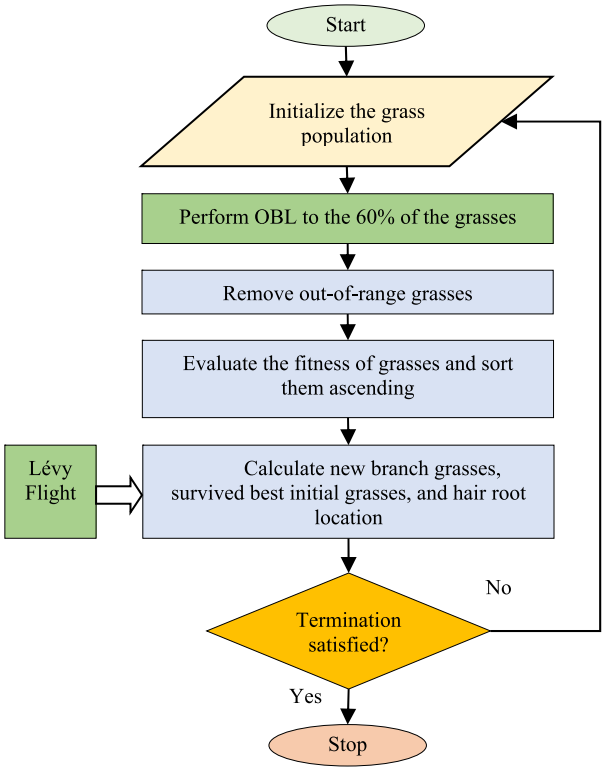

Fig. 2. The flowchart diagram of the proposed IGRA.

$$w = A \times |B|^{-\left(\frac{1}{\tau}\right)} \tag{47}$$

$$\sigma^2 = \left\{\frac{\sin(\pi \times \tau/2)}{2^{(1+\tau)/2}} \times \frac{\Gamma(1+\tau)}{\tau \times \Gamma((1+\tau)/2)}\right\}^{2\tau^{-1}} \tag{48}$$

where, w describes the step size, τ stands for the LF index (her, $\tau = 1.5$) (Li et al., 2018), $A \sim N(0, \sigma^2)$, $B \sim N(0, \sigma^2)$, and $\Gamma(.)$ indicates the Gamma function.

By considering the above assumptions, the updated formula for the new branch grasses, survived best initial grasses, and hair root location are consequently as follows:

$$Gr_N^+ = ones(Gr, 1) \times G_{best} + 2 \times \mathrm{LF}(\delta) \times \max\left(Pop_{New}^H\right) \times (\sigma(Gr, 1) - 0.5) \times G_{best} \tag{49}$$

$$S_{de}^+ = Gr_N + 2 \times \max\left(Pop_{New}^H\right) \times \mathrm{LF}(\delta) \times (\sigma(pop\text{–}Gr - 1, 1) - 0.5) \times Pop_{New}^H \tag{50}$$

$$m_{G_{best}}(1,i) = Avg(G_{best}) + G_{best}(1,i) + C_2 \times \mathrm{LF}(\delta) \times (\sigma - 0.5) \tag{51}$$

Fig. 2 indicates the flowchart diagram of the presented IGRA.

3.3. The performance verification of the proposed algorithm

To verify the efficiency of the presented IGRA, some benchmark functions have been adopted and the results compared with some other optimization algorithms from the literature. The iteration number for all the algorithms is considered 100. The compared algorithms are States of Matter (SMS) (Cuevas et al., 2020), Lion Optimization Algorithm (LOA) (Yazdani and Jolai, 2016), Thermal Exchange Optimization (TEO) (Kaveh and Dadras, 2017), Socio Evolution and Learning Optimization Algorithm (SELO) (Kumar et al., 2018), and the basic Grass Fibrous Root Optimization Algorithm (GRA) (Cuevas et al., 2018). The formulation for the adopted test functions has been explained

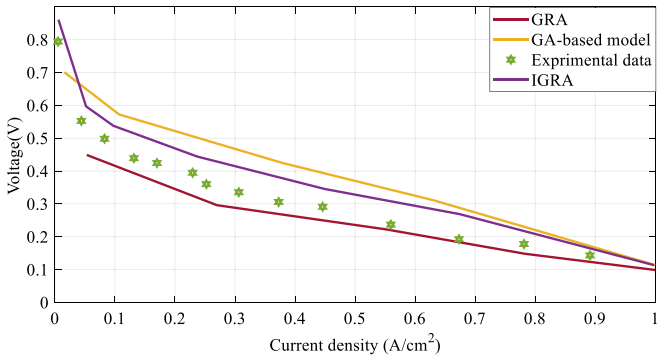

Fig. 3. The polarization diagram for the analyzed algorithms with considering P = 1 and T = 199.85 °C.

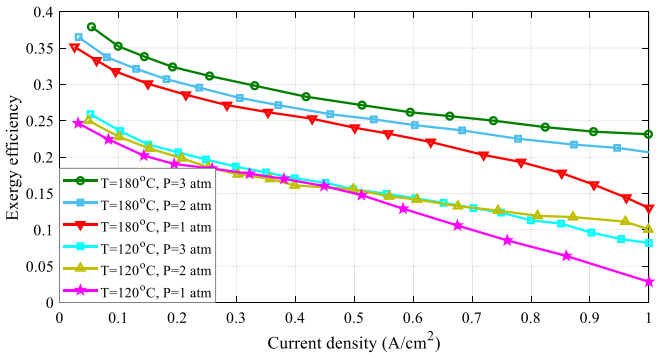

Fig. 4. The impact of pressure and temperature on the exergy performance.

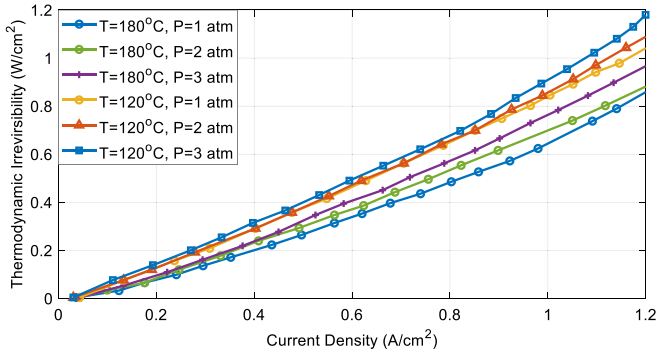

Fig. 5. The simulation results for the thermodynamic irreversibility toward the current density.

below:

$$F_1(x) = \sum_{i=1}^{D-1} \left(100\left(x_i^2 - x_{i+1}\right) + (x_i - 1)^2\right) \tag{52}$$

$$F_2(x) = \sum_{i=1}^{D} x_i^2 \tag{53}$$

$$F_3(x) = 10D + \sum_{i=1}^{D} \left(x_i^2 - 10cos\left(2\pi x_i\right)\right) \tag{54}$$

$$F_4(x) = -20exp\left(-0.2\sqrt{\frac{1}{D}\sum_{i=1}^{D}\left(x_i^2\right)}\right) - exp\left(\frac{1}{D}\sum_{i=1}^{D}\left(cos\left(2\pi x_i\right)\right)\right) + 20 + e \tag{55}$$

In the above equations, F_1 is the *Rosenbrock* function that is restricted in the range $[-2.045, 2.045]$, F_2 and F_3 describe the *Sphere* function and the *Rastrigin* function in the range in the interval $[-512, 512]$, respectively, and F_4 determines the *Ackley* function in the interval $[-10, 10]$.

Table 2 shows the median value (MV) and the standard deviation value (SD) for the algorithms. As can be observed, the value of both MV and SD for the proposed IGRA is lower than the other compared algorithms which shows its higher accuracy and precision toward the others.

4. Simulation results

This section presents the results and the discussion of the parametric studies using the mathematical model in details. The performance assessment parameters are taken as fuel cell irreversibility, exergy efficiency, and its work. To analyze of the proposed system efficiency, it is simulated based on Matlab Simulink software. The method is first coded and simulated in the Matlab platform and then, its results are compared with some other methods including Genetic Algorithm (GA) (Haghighi and Sharifhassan, 2016), the basic Grass Fibrous Root Optimization Algorithm (GRA) (Cuevas et al., 2018), and also the experimental results extracted from Ubong data (Ubong et al., 2009). The polarization diagram for the analyzed algorithms with considering $T = 199.85°C$ and P=1 is given in Fig. 3. Indeed, Fig. 3 shows the performance of PEMFC by different algorithms. The cell performance is slightly improved from IGRA to GA based method, but it is clear that the best state for the real output among the all compared methods is the suggested IGRA.

As it is clear, the proposed IGRA gives the best fittest results to the empirical data. This can be observed in Fig. 4. As can be seen, by assuming the constant membrane thickness of 0.017 cm, enhancing the current density makes the efficiency of the exergy to get decreased, while enhancing the temperature increases the efficiency of the exergy.

As can be observed, increasing the temperature makes a sensible rising on the mass exergy and the $\dot{W}_{FC}$ of the feed and consequently the ratio of $\dot{W}_{FC}/Ex^{in}_{mass}$. Here, the effect of the pressure on the exergy efficiency has been neglected. More analysis has been done by analyzing the thermodynamic irreversibility that is determined by the input and the output consumed exergy and work. The simulation results for the thermodynamic irreversibility ($\dot{I}_{FC}$) toward the current density have been shown by different pressure and temperature values in Fig. 5. As can be seen, the more the current density value increased, the more the thermodynamic irreversibility value increases. Figure also shows that at the same temperature, the thermodynamic irreversibility is proportional to the pressure.

The study also analysis the effect of membrane thickness and the current densities changes on the exergy efficiency. Fig. 6 gives the simulation results for the effect of the membrane thickness variations on the exergy efficiency by operating pressure fixed on 3 atm. As it is clear from Fig. 6, increasing of the temperature makes the exergy efficiency increasing. Besides, due to the increasing of $E\dot{x}_{mass,in}$ which makes the work decreasing to input exergy ratio, increasing the current density, enhances the thermodynamic irreversibility.

In this study, 3 single-objective optimizations are adopted for the system and the results are optimized by the proposed IGRA. Table 3 indicates the feasible range of parameters for the studied system (Akkar and Mahdi, 2017). Based on Akkar and Mahdi (2017), the pressure of the system is considered in the range 1

Table 2
The numerical results of the analyzed algorithms on the adopted functions.

Benchmark		IGRA	GRA (Cuevas et al., 2018)	LOA (Yazdani and Jolai, 2016)	SMS (Cuevas et al., 2020)	SELO (Kumar et al., 2018)	SMS (Cuevas et al., 2020)
F_1	MV	0.00	0.00	1.42e−4	4.38e−4	1.17e−9	0.00
	SD	0.00	0.00	4.29e−5	9.44e−4	5.24e−9	0.00
F_2	MV	4.28	5.16	52.45	42.15	12.30	11.85
	SD	2.86	5.19	32.08	40.25	4.92	6.34
F_3	MV	0.00	2.12	30.11	45.27	10.52	3.82
	SD	0.00	1.50	7.25	15.46	4.83	3.17
F_4	MV	0.00	2.89e−17	4.62e−2	7.41	3.98e−4	4.86e−16
	SD	0.00	0.00	3.72e−2	3.83	3.15e−4	0.00

Table 3
The Optimization results of the Irreversibility, Work, and Exergy efficiency.

The objective Function	Current density (A/cm^2)	Pressure (atm)	The fitness value (W/cm^2)		
			GA	GRA	IGRA
Irreversibility	0.06	3	0.015	0.012	0.012
Work	1	2	−0.4490	−0.4899	−0.4993
Exergy efficiency	0.06	3	−0.437	−0.439	−0.439

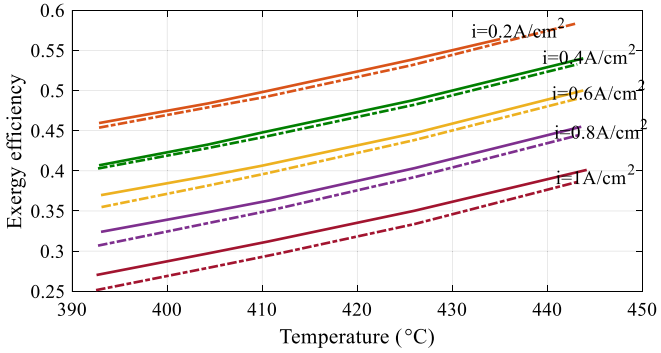

Fig. 6. The simulation results for the temperature toward exergy efficiency during the membrane thickness variations.

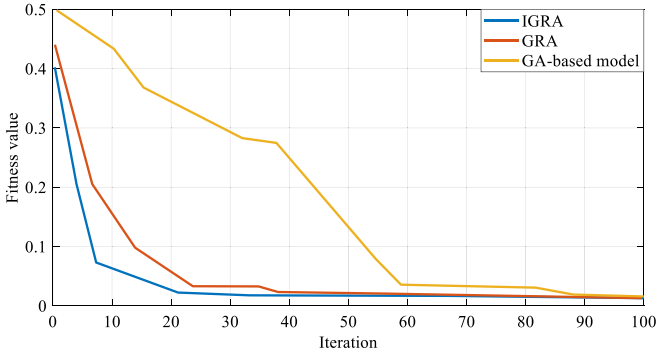

Fig. 7. The convergence diagram of the fitness for the irreversibility term.

atm and 3 atm, temperature is limited in the range 125 °C and 185 °C, current density is considered in the interval 0.05 A/cm^2 and 1.3 A/cm^2, and membrane thickness is limited between 0.02 cm and 0.03 cm.

In this research, the population size and the number of iterations for all the algorithms are considered 100, the mutation rate is considered 0.6, the crossover rate is assumed 0.4, and $\varepsilon = 0.02$. It should be note that the parameters values for the optimization are achieved based on trials and error.

Table 3 illustrates the final results of applying the analyzed algorithms on the fitness functions. These results have been obtained for the PEMFC with 0.018 cm membrane thickness at 180 °C.

The current density and pressure of the objective functions are supposed similar to each other. The results show higher efficiency with $-0.4993 W/cm^2$ for the proposed IGRA. Furthermore, the irreversibility value is 0.012 W/cm^2 which is achieved by the GRA and the suggested IGRA and shows the system efficiency. Also, exergy efficiency for the suggested IGRA is the best compared with the GA.

For more clarification, the results of the fitness value for irreversibility, work, and exergy efficiency functions are given in Fig. 7–Fig. 9, respectively.

The irreversibility convergence of the system is given in Fig. 7. It is obvious that the presented algorithm gives the minimum value with minimum iteration for the convergence (35 iterations). More information about this optimization is given in Table 3. Table declares that the value of the irreversibility at iteration 100 is 0.012 w/cm^2 that is a proper performance for the results.

As it is clear from Fig. 8, single-objective optimization of the work term diagram, the best minimum value and the best convergence is achieved by the proposed IGRA that is converges in iteration 33 toward the GA that gives the worst result with larger convergence steps that in iteration 100. The prominent ability of the proposed algorithm in convergence than the basic GRA is obvious from the diagram.

Finally, the optimal efficiency for the exergy of the system is analyzed based on its convergence. The details of this term are illustrated in Table 3 and Fig. 9. As can be seen, the GRA based algorithms has better results than the GA for exergy efficiency, however, the presented IGRA has faster convergence to the fixed value toward the others (iteration 62).

5. Conclusion

Among different new generation systems, fuel cell-based systems are a good option for cogeneration for reasons such as high

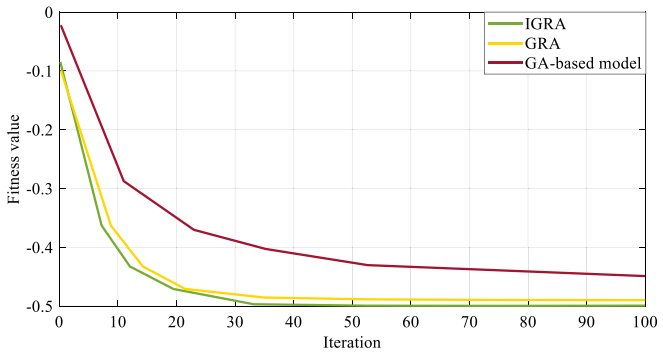

Fig. 8. The convergence diagram of the fitness for the work term.

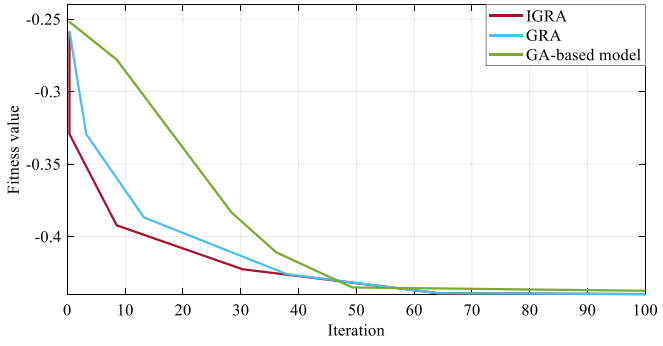

Fig. 9. The convergence diagram of the fitness for the exergy efficiency.

efficiency and power density, pollution and low noise. Proton-exchange membrane fuel cell (PEMFC), especially the high temperature type of that is one of the highest performance types of fuel cells that has lots of applications in the recent decade. In this study, an exergy analysis was proposed to a high-temperature PEMFC. For achieving an optimal steady-state model, some parameters were optimized. The optimization process was applied using a new modified Grass Fibrous Root Optimization Algorithm (IGRA). After validation of the presented optimization algorithm by comparing it with some metaheuristics to show its prominence features, it was utilized for optimizing the PEMFC system. The system was then utilized for analyzing three primary terms including irreversibility, work, and exergy efficiency. The results showed that with considering the constant membrane thickness of 0.017 cm, enhancing the current density decreases the exergy efficiency, while enhancing the temperature gives sensible rising on the exergy efficiency, mass exergy and the $\dot{W}_{FC}$ of the feed and consequently the ratio of $\dot{W}_{FC}/\dot{E}x^{in}_{mass}$. The results also showed that by increasing the $\dot{Ex}_{mass,in}$, decreases the input exergy ratio and increases the current density and thermodynamic irreversibility and at the same temperature, the thermodynamic irreversibility is proportional to the pressure. Results showed that for single-objective optimization of the work term diagram among different algorithms, the suggested IGRA gives the best optimum value and the fastest convergence toward the others in iteration 33. The prominent ability of the proposed algorithm in convergence than the basic GRA is obvious from the diagram. The simulation results were compared with empirical data, basic GRA, and also GA and the evaluations indicated that IGRA gives the best results for the exergy analysis. In the future work, the system will be analyzed by considering different uncertainties. These uncertainties will be including different stochastic models which will be performed based on stochastic formulations.

CRediT authorship contribution statement

Xiaohui Lu: Conceptualization, Data curation, Writing - original draft, Writing - review & editing. **Jianglin Ren:** Conceptualization, Data curation, Writing - original draft, Writing - review & editing. **Lin Guo:** Conceptualization, Data curation, Writing - original draft, Writing - review & editing. **Peifang Wang:** Conceptualization, Data curation, Writing - original draft, Writing - review & editing. **Nasser Yousefi:** Conceptualization, Data curation, Writing - original draft, Writing - review & editing.

Declaration of competing interest

The authors declare that they have no known competing financial interests or personal relationships that could have appeared to influence the work reported in this paper.

Acknowledgments

This study was financed by the National Natural Science Foundation of China (Grant No. 51979078); The Fundamental Research Funds for Central Universities, China.

References

Aghajani, Gholamreza, Ghadimi, Noradin, 2018. Multi-objective energy management in a micro-grid. Energy Rep. 4, 218–225.
Akbary, Paria, et al., 2019. Extracting appropriate nodal marginal prices for all types of committed reserve. Comput. Econ. 53 (1), 1–26.
Akkar, H.A., Mahdi, F.R., 2017. Grass fibrous root optimization algorithm. Int. J. Intell. Syst. Appl. 11 (6), 15.
Alberro, M., Marzo, F., Manso, A., Domínguez, V., Barranco, J., Garikano, X., 2015. Electronic modeling of a PEMFC with logarithmic amplifiers. Int. J. Hydrogen Energy 40 (9), 3708–3718.
Amphlett, J.C., Baumert, R.M., Mann, R.F., Peppley, B.A., Roberge, P.R., Harris, T.J., 1995. Performance modeling of the Ballard Mark IV solid polymer electrolyte fuel cell I. Mechanistic model development. J. Electrochem. Soc. 142 (1), 1–8.
Bandaghiri, P.S., Moradi, N., Tehrani, S.S., 2016. Optimal tuning of PID controller parameters for speed control of DC motor based on world cup optimization algorithm. Parameters 1, 2.
Berning, T., Lu, D., Djilali, N., 2002. Three-dimensional computational analysis of transport phenomena in a PEM fuel cell. J. Power Sources 106 (1–2), 284–294.
Chang, H., Duan, C., Xu, X., Pei, H., Shu, S., Tu, Z., 2019. Technical performance analysis of a micro-combined cooling, heating and power system based on solar energy and high temperature PEMFC. Int. J. Hydrogen Energy 44 (38), 21080–21089.
Choi, C., Lee, J.-J., 1998. Chaotic local search algorithm. Artif. Life Robot. 2 (1), 41–47.
Cuevas, E., Fausto, F., González, A., 2020. A swarm algorithm inspired by the collective animal behavior. In: New Advancements in Swarm Algorithms: Operators and Applications. Springer, pp. 161–188.
Cuevas, E., Reyna-Orta, A., Díaz-Cortes, M.-A., 2018. A multimodal optimization algorithm inspired by the states of matter. Neural Process. Lett. 48 (1), 517–556.
Cui, Z., et al., 2019. A pigeon-inspired optimization algorithm for many-objective optimization problems. Sci. China Inf. Sci. 62, 070212.
Dhiman, G., Kumar, V., 2018. Emperor penguin optimizer: A bio-inspired algorithm for engineering problems. Knowl.-Based Syst. 159, 20–50.
Ebrahimian, Homayoun, et al., 2018. The price prediction for the energy market based on a new method. Econ. Res.-Ekon. Istraživanja 31 (1), 313–337.
Ehyaei, M., Rosen, M.A., 2019. Optimization of a triple cycle based on a solid oxide fuel cell and gas and steam cycles with a multiobjective genetic algorithm and energy, exergy and economic analyses. Energy Convers. Manag. 180, 689–708.
Eskandari Nasab, M., Maleksaeedi, I., Mohammadi, M., Ghadimi, N., 2014. A new multiobjective allocator of capacitor banks and distributed generations using a new investigated differential evolution. Complexity 19 (5), 40–54.
Fan, X., Sun, H., Yuan, Z., Li, Z., Shi, R., Razmjooy, N., 2020. Multi-objective optimization for the proper selection of the best heat pump technology in a fuel cell-heat pump micro-CHP system. Energy Rep. 6, 325–335.
Fei, X., Xuejun, R., Razmjooy, N., 2019. Optimal configuration and energy management for combined solar chimney, solid oxide electrolysis, and fuel cell: a case study in Iran. Energy Sources A: Recovery Util. Environ. Eff. 1–21.

Gao, W., Darvishan, A., Toghani, M., Mohammadi, M., Abedinia, O., Ghadimi, N., 2019. Different states of multi-block based forecast engine for price and load prediction. Int. J. Electr. Power Energy Syst. 104, 423–435.
Ghadimi, N., 2012. Genetically tuning of lead–lag controller in order to control of fuel cell voltage. Sci. Res. Essays 7 (43), 3695–3701.
Gollou, Abbas Rahimi, Ghadimi, Noradin, 2017. A new feature selection and hybrid forecast engine for day-ahead price forecasting of electricity markets. J. Intell. Fuzzy Systems 32 (6), 4031–4045.
Haghighi, M., Sharifhassan, F., 2016. Exergy analysis and optimization of a high temperature proton exchange membrane fuel cell using genetic algorithm. Case Stud. Therm. Eng. 8, 207–217.
Hamian, Melika, et al., 2018. A framework to expedite joint energy-reserve payment cost minimization using a custom-designed method based on Mixed Integer Genetic Algorithm. Eng. Appl. Artif. Intell. 72, 203–212.
Hosseini Firouz, Mansour, Ghadimi, Noradin, 2016. Optimal preventive maintenance policy for electric power distribution systems based on the fuzzy AHP methods. Complexity 21 (6), 70–88.
Ishihara, A., Mitsushima, S., Kamiya, N., Ota, K.-i., 2004. Exergy analysis of polymer electrolyte fuel cell systems using methanol. J. Power Sources 126 (1–2), 34–40.
Kaveh, A., Dadras, A., 2017. A novel meta-heuristic optimization algorithm: thermal exchange optimization. Adv. Eng. Softw. 110, 69–84.
Kumar, M., Kulkarni, A.J., Satapathy, S.C., 2018. Socio evolution & learning optimization algorithm: A socio-inspired optimization methodology. Future Gener. Comput. Syst. 81, 252–272.
Kwon, O.-J., Shin, H.-S., Cheon, S.-H., Oh, B.S., 2015. A study of numerical analysis for PEMFC using a multiphysics program and statistical method. Int. J. Hydrogen Energy 40 (35), 11577–11586.
Lee, W.-Y., Park, G.-G., Yang, T.-H., Yoon, Y.-G., Kim, C.-S., 2004. Empirical modeling of polymer electrolyte membrane fuel cell performance using artificial neural networks. Int. J. Hydrogen Energy 29 (9), 961–966.
Leng, Hua, et al., 2018. A new wind power prediction method based on ridgelet transforms, hybrid feature selection and closed-loop forecasting. Adv. Eng. Inform. 36, 20–30.
Li, X., Niu, P., Liu, J., 2018. Combustion optimization of a boiler based on the chaos and Levy flight vortex search algorithm. Appl. Math. Model. 58, 3–18.
Liu, Yang, Wang, Wei, Ghadimi, Noradin, 2017. Electricity load forecasting by an improved forecast engine for building level consumers. Energy 139, 18–30.
Liu, Jun, et al., 2020. An IGDT-based risk-involved optimal bidding strategy for hydrogen storage-based intelligent parking lot of electric vehicles. J. Energy Storage 27, 101057.
Mirzapour, Farzaneh, et al., 2019. A new prediction model of battery and wind-solar output in hybrid power system. J. Ambient Intell. Humaniz. Comput. 10 (1), 77–87.
Razmjooy, N., Madadi, A., Ramezani, M., 2017. Robust control of power system stabilizer using world cup optimization algorithm. Int. J. Inf. Secur. Syst. Manag. 5 (1), 7.
Razmjooy, N., Ramezani, M., 2014. An improved quantum evolutionary algorithm based on invasive weed optimization. Indian J. Sci. Res. 4 (2), 413–422.
Reddy, E.H., Jayanti, S., 2012. Thermal management strategies for a 1 kWe stack of a high temperature proton exchange membrane fuel cell. Appl. Therm. Eng. 48, 465–475.
Rowe, A., Li, X., 2001. Mathematical modeling of proton exchange membrane fuel cells. J. Power Sources 102 (1–2), 82–96.
Saeedi, M., Moradi, M., Hosseini, M., Emamifar, A., Ghadimi, N., 2019. Robust optimization based optimal chiller loading under cooling demand uncertainty. Appl. Therm. Eng. 148, 1081–1091.
Shahrezaee, M., 2017. Image segmentation based on world cup optimization algorithm. Majlesi J. Electr. Eng. 11 (2).
Shamel, A., Ghadimi, N., 2016. Hybrid PSOTVAC/BFA technique for tuning of robust PID controller of fuel cell voltage.
Springer, T.E., Zawodzinski, T., Gottesfeld, S., 1991. Polymer electrolyte fuel cell model. J. Electrochem. Soc. 138 (8), 2334–2342.
Tian, M.-W., Yan, S.-R., Han, S.-Z., Nojavan, S., Jermsittiparsert, K., Razmjooy, N., 2020. New optimal design for a hybrid solar chimney, solid oxide electrolysis and fuel cell based on improved deer hunting optimization algorithm. J. Cleaner Prod. 249, 119414.
Tizhoosh, H.R., 2005. Opposition-based learning: a new scheme for machine intelligence. In: International Conference on Computational Intelligence for Modelling, Control and Automation and International Conference on Intelligent Agents, Web Technologies and Internet Commerce, Vol. 1. CIMCA-IAWTIC'06, IEEE, pp. 695–701.
Ubong, E., Shi, Z., Wang, X., 2009. Three-dimensional modeling and experimental study of a high temperature PBI-based PEM fuel cell. J. Electrochem. Soc. 156 (10), B1276–B1282.
Yazdani, M., Jolai, F., 2016. Lion optimization algorithm (LOA): a nature-inspired metaheuristic algorithm. J. Comput. Design Eng. 3 (1), 24–36.
Yu, Dongmin, Ghadimi, Noradin, 2019. Reliability constraint stochastic UC by considering the correlation of random variables with Copula theory. IET Renew. Power Gener. 13 (14), 2587–2593.